IEEE Access
Multidisciplinary ⋮ Rapid Review ⋮ Open Access Journal

Date of publication xxxx 00, 0000, date of current version xxxx 00, 0000.

Digital Object Identifier 10.1109/ACCESS.2024.Doi Number

A Novel Unified Single-Phase Active Rectifier Topology with Advanced Operating Modes for Smart Grids

Vitor Monteiro[1], (Senior Member, IEEE), Filipe Costa[1], Sergio Coelho[1], (Student Member, IEEE) and Joao L. Afonso[1], (Senior Member, IEEE)

[1] Centro ALGORITMI / LASI, University of Minho, Portugal

Corresponding author: Vitor Monteiro (e-mail: vmonteiro@dei.uminho.pt)

This paragraph of the first footnote will contain support information, including sponsor and financial support acknowledgment. For example, "This work was supported in part by the U.S. Department of Commerce under Grant BS123456."

ABSTRACT Active rectifiers are of paramount importance for guaranteeing power quality in smart grids, due to their characteristics of sinusoidal current consumption and unitary power factor operation. In this paper, a novel unified single-phase (USP) front-end converter is proposed for active rectifier applications in smart grids, offering additional advantages and a set of relevant features besides the conventional active rectification. With the proposed USP front-end converter, the following independent operation modes are available: (i) operation as a traditional active rectifier, ensuring sinusoidal AC grid current (with very low total harmonic distortion), unitary power factor, and controlled DC link voltage; (ii) operation as a shunt active power filter, producing a current with controlled harmonic content and phase angle at the fundamental frequency, in order to ensure almost sinusoidal current and a unitary power factor at the AC power grid; (iii) combined operation as an active rectifier and as a shunt active power filter, providing power to the DC load, while simultaneously producing a current waveform with reduced harmonic content and controlled power factor. By controlling these individual operation modes, electrical appliances in smart grids can operate dynamically and collaboratively, improving power quality. In addition, the proposed USP front end converter may operate as a single-phase diode rectifier in case of control system failure or damage of the controlled switching devices. This situation is particularly relevant since it allows to supply the DC load even under such unfortunate circumstances. Along with the paper, the topology of the proposed USP front end converter, its principle of operation, and the control strategies for each operation mode, are separately explained. A 3.6 kW, 230 V – 50 Hz laboratorial prototype of the proposed USP front end converter is presented, and the experimental validation is carried out for all operation modes.

INDEX TERMS Active Rectifier, Active Power Filter, Power Quality, Single-Phase, Smart Grid

I. INTRODUCTION

The pioneering model of smart grids is indisputably influenced by the existence of newfound technologies, e.g., electric mobility and renewables, aiming to address environmental and sustainable matters, but at the same time, they also introduce an unpredictable behavior [1], [2], and pose significant challenges, such as cybersecurity risks [3]. In addition, as an imperative feature given their power profile, such technologies must not negatively impact the power quality [4], [5], even when operating in a multifunctional cooperation [6], or with on-board/off-board EV chargers [7], [8]. Thus, a customary contribution to diminish the poor power quality regarding reactive power and current harmonics, consists in the substitution of the old passive AC-DC rectifiers by active rectifiers [9], [10]. As the name implies, active rectifiers offer controllability regarding the AC current, driving the operation with sinusoidal current and unitary power factor. This is feasible to reach by employing distinct topologies of power converters, where the most widespread and simple to control is the boost configuration [11], [12], however new topologies are identified [13], [14]. Although classified as a front-end converter, it is categorized by the internal constitution of two power stages: a passive AC-DC rectifier and a controlled DC-DC converter. Consequently, all

the power delivered to the DC load is processed by these two power stages. Opportunely, other topologies can be used, namely the bridgeless topologies, which are categorized by the absence of the AC-DC passive rectifier [15], [16]. Despite the indubitable benefits of the active rectifiers, they are solely used for ensuring sinusoidal current and unitary power factor on the AC side and controlled DC-link voltage on the DC side. However, by considering the real context of smart grids, it can be valuable to add additional features to the active rectifiers, without jeopardizing its main principle of operation, but providing benefits to the smart grid.

Thus, aligned with this thematic, this paper proposes a novel unified single-phase (USP) front-end converter designed to operate in multiple modes: (i) as a traditional active rectifier; (ii) as a shunt active power filter; and (iii) in combined operation, as an active rectifier and as a shunt active power filter. The context and the topology of the proposed USP front-end converter is shown in FIGURE 1, which is composed by two main parts, namely a diode full-bridge converter (formed by the diodes d_1 to d_4), named as full-wave rectifier (FWR), and by a full-controlled full-bridge converter (formed by the IGBTs g_1 to g_4), named as bidirectional active rectifier (BAR). The BAR has an intermediary DC-link (C_1), while the FWR contains a DC-link interface (C_2) for a DC-DC back-end converter or for a direct connection with a DC load. A common-mode inductive filter is used to couple the USP front-end converter with the AC power grid.

The possibility of combining different features and technologies, either through several power converters or by integrating them into a single-stage solution, has already been identified and validated in the literature. For instance, a single-phase interface between distributed generation and a shunt active power filter is presented in [17]. Although it relies on two distinct power converters, its main contribution is the implementation of a neural control strategy. A combined three-phase series-shunt active power filter with a power converter connected in the DC-link to interface a solar photovoltaic system is presented in [18], permitting the operation with active/reactive power control through the shunt filter. Nonetheless, the solution requires three distinct power converters and does not provide a DC interface. A similar structure is proposed in [19], but without a power converter to interface the solar photovoltaic system. This reduces hardware complexity but limits the system's operational flexibility. In contrast, a hybrid DC interface combining battery storage and solar photovoltaic systems is presented in [20], enabling active/reactive power control through the shunt converter. However, this approach requires additional converters and lacks redundancy. An analogous design is proposed in [21] for three-phase applications, but its main drawback lies in the impossibility of controlling the output DC-link voltage. In addition, similar structures can be implemented aiming for the improvement of power quality, while also offering the possibility of operating with bidirectional active power. Therefore, both single-phase and three-phase systems are

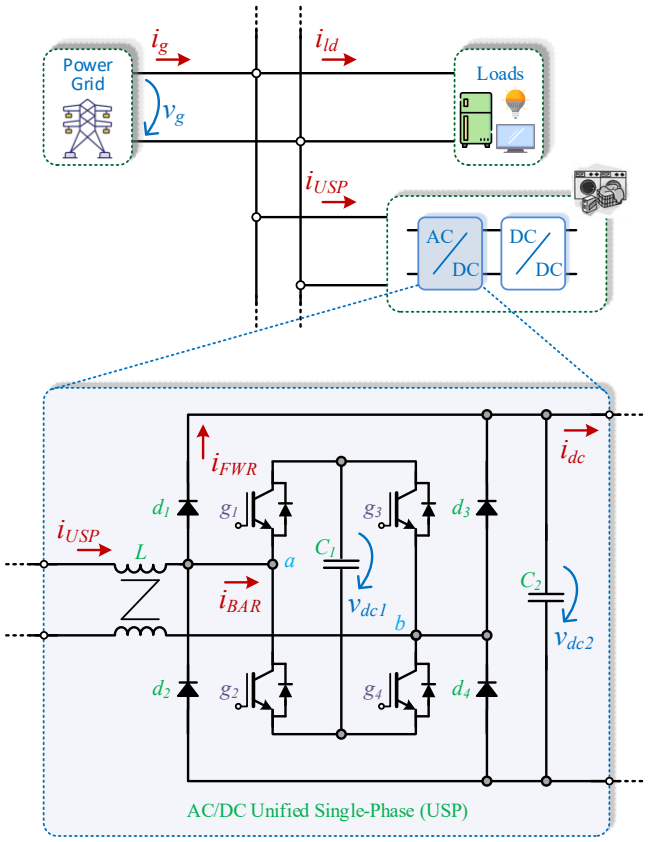

FIGURE 1. Proposed unified single-phase (USP) front-end converter.

identified, targeting the compensation or attenuation of current harmonics, the combined mitigation of voltage and current, and in some cases, reactive power compensation. Normally, these solutions employ full-bridge topologies, cascade arrangements, or other innovative power converter structures, as presented in [22]-[29]. Thus, it is recognized the possibility of combining features of active rectifiers with active power filters, which is of utmost importance. A comprehensive comparison is presented in TABLE I, covering the previously discussed approaches. It includes the different types of application considered, the topology of power electronics converters used, their integration context, and the corresponding compensation capabilities. Supported by the analysis of the identified benefits and drawbacks, the distinguished features of the proposed USP front-end converter are described as follows:

1. Operation in three distinct modes, allowing to respond to the power needs of the DC side, as well as to provide add-value functions to the smart grid, namely: (a) operation as a traditional active rectifier, receiving power from the grid and ensuring sinusoidal AC current and unitary power factor; (b) operation as a shunt active power filter, just producing reactive power and current harmonics to the power grid for ensuring sinusoidal current and unitary power factor in the common coupling point; (c) combined operation of both previous cases, providing power to the DC side, while operating as a shunt active power filter, compensating current

TABLE I. Comprehensive comparison, including the different types of application, the topology of power electronics converters used and respective contextualization of integration, as well as the compensation operation.

	Application	Topology	Compensation
[17]	Distributed generation interfacing renewables through the dc-link	Single-phase full-bridge in a shunt power filter	Current harmonics and reactive power
[18]	Interfacing solar PV in the DC-link without additional converters	Three-phase full-bridge in a unified power quality conditioner	Current harmonics and reactive power
[19]	Interfacing solar PV in the DC-link with additional DC-DC converter	Three-phase full-bridge in a unified power quality conditioner	Current harmonics and reactive power
[20]	Interfacing battery storage and solar PV in the DC-link without additional converters	Three-phase full-bridge in a unified power quality conditioner	Current harmonics and reactive power
[21]	EV battery chargers, including an additional DC-DC power converter	Three-phase swiss rectifier in a shunt power filter	Current harmonics and reactive power
[22]	Interfacing battery storage and solar PV in the DC-link with additional converters	Three-phase full-bridge in a unified power quality conditioner	Current harmonics and reactive power
[23]	Interfacing battery storage and solar PV in the DC-link with additional converters	Three-phase full-bridge in a universal active power filter	Current harmonics and reactive power
[24]	Interfacing solar PV in the DC-link with additional DC-DC converter	Three-phase full-bridge in a universal active power filter	Current harmonics and reactive power
[25]	Interfacing solar PV in the DC-link without additional DC-DC converter	Three-phase full-bridge in a shunt power filter	Partial current harmonic compensation
[26]	Interfacing solar PV in the DC-link without additional DC-DC converter	Single-phase full bridge in a series/shunt power filter	Current harmonics and reactive power
[27]	Interfacing EV with additional DC-DC converter	Single-phase totem-pole boost power factor correction	Current harmonics reduction
[28]	Interfacing EV and solar PV in the DC-link with additional converters	Three-phase full-bridge in a shunt power filter	Reactive power compensation
[29]	Interfacing EV, battery storage and solar PV in the DC-link with additional converters	Three-phase Cascade full-bridge in a shunt active power filter	Current harmonics and reactive power

harmonics and reactive power of the non-linear loads in the same installation. 2. Even in the case of a failure of the BAR, it is possible to provide power to the DC side through the FWR, which is an intermediate and preferable compromise solution than not feeding the DC side, as happens in a traditional converter. 3. Controlled current on the AC power grid, but with internal current separation, i.e., the AC current (i_{USP}) from the AC power grid is divided into two parcels, the FWR current (i_{FWR}) and the BAR current (i_{BAR}), allowing to reduce switching losses. 4. Controlled DC-link voltage in all operation modes, like a traditional active rectifier front-end converter and where it can be connected a DC-DC back-end converter or a DC load. 5. Experimental validation of all the previous cases, both in steady-state and transient-state, with a full developed laboratory prototype, specifically designed for such purpose, and tested directly plugged-in into the 230 V AC power grid without any controlled power source.

The characterization of the proposed USP front-end converter framed with its advanced operation modes in smart grids is introduced in section II. An explanation of the proposed control algorithm for the distinct operations is presented in section III. The experimental setup and respective validation of the referred operation modes are exposed in section IV. Finally, conclusions are given in section V.

II. PROPOSED UNIFIED FRONT-END CONVERTER: PRINCIPLE OF OPERATION

A detailed description of the proposed USP front-end converter is presented in this section, highlighting the different and independent operation modes. FIGURE 2 visually explains the operation of the USP front-end converter across the three different operating modes. FIGURE 2(a) illustrates the operation as a traditional active rectifier, ensuring sinusoidal AC grid current (with very low total harmonic distortion), unitary power factor, and controlled DC link voltage. FIGURE 2(b) illustrates the operation as a shunt active power filter, producing a current with controlled harmonic content and phase angle at the fundamental frequency, to ensure almost sinusoidal current and a unitary power factor at the AC power grid. Finally, FIGURE 2(c) illustrates the combined operation as an active rectifier and as a shunt active power filter, providing power to the DC load, while simultaneously producing a

current waveform with reduced harmonic content and controlled power factor.

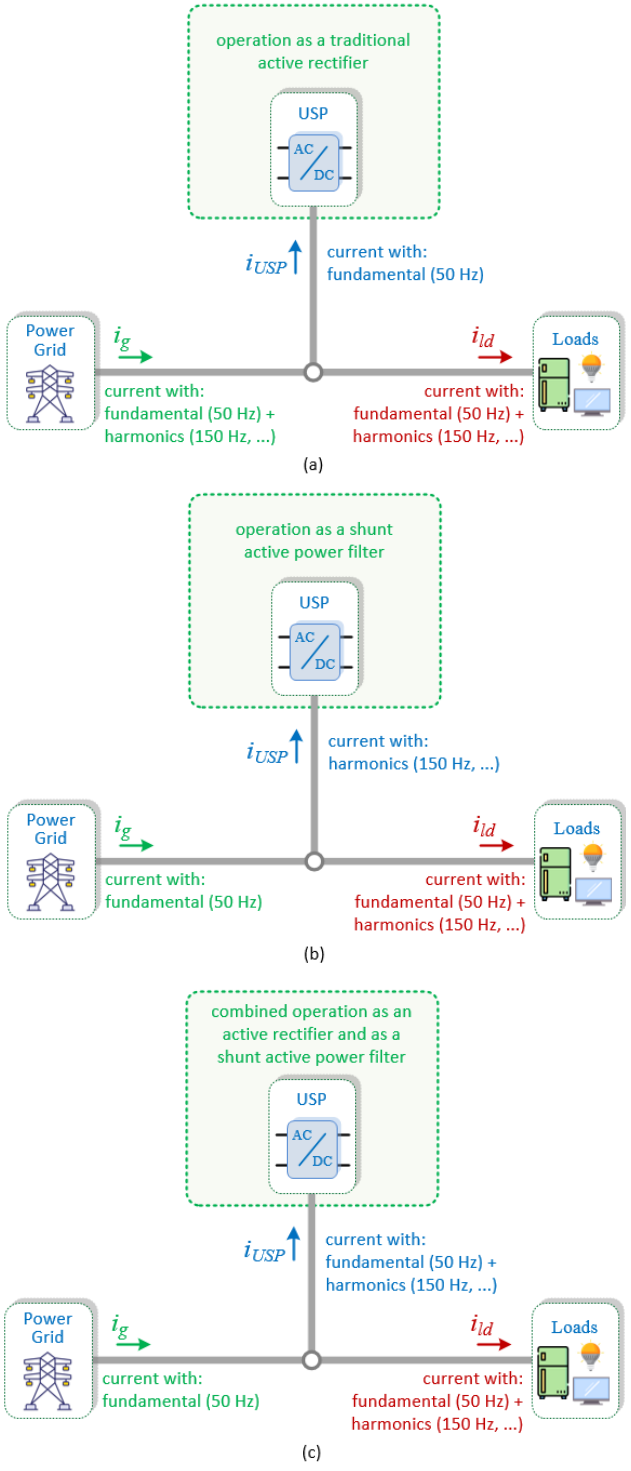

FIGURE 2. Operation of the USP front-end converter across the three different operating modes: (a) Operation as a traditional active rectifier; (b) Operation as a shunt active power filter; (c) Combined operation as an active rectifier and as a shunt active power filter.

A. Operation Mode: Active Rectifier

The main purpose of an active rectifier is related to the AC side, forcing the operation with sinusoidal current and unitary power factor. In this mode, the power is provided by the AC power grid to the DC side through the USP front-end converter, which also controls the DC-link voltage, so that the back-end converter can properly control the voltage and current levels for the DC load. In this operation mode, the USP front-end converter operates with sinusoidal current and unitary power factor, however, since non-linear loads are connected in the same electrical installation, the main current in the power grid, which is the sum of the currents, present harmonic content, and the power grid exchanges reactive power. This situation is illustrated in FIGURE 3.

Any topology of active rectifier needs to establish a proper synchronization with AC voltage to control the desired current. Consequently, a phase-locked loop (PLL) algorithm is used to extract the fundamental component of the AC voltage [30]. This algorithm is not only used to achieve synchronization but also to accomplish the generation of a sinusoidal AC reference current in the presence of a non-sinusoidal AC voltage. In fact, this corresponds to the actual situation of the AC voltage nowadays, which presents harmonic distortion. By using the fundamental component of the AC voltage instead of its total value, i.e., not including the harmonic content, it is possible to achieve a sinusoidal AC current, thereby the USP front-end converter only operates just with active power. Otherwise, the harmonic content of the AC current would be the same as the harmonic content of the AC voltage, which would cause the converter to operate with harmonic power.

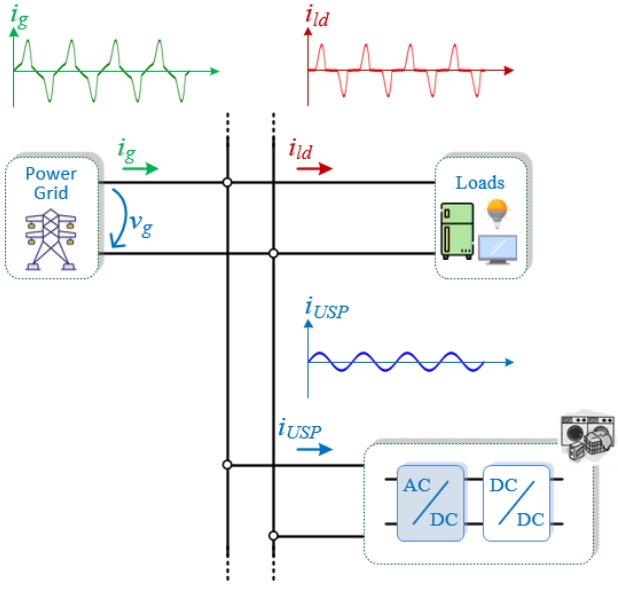

FIGURE 3. Operation mode of the USP front-end converter as active rectifier, where it operates with sinusoidal current and unitary power factor (i_{USP}), but due to the non-linear loads in the same electrical installation (i_{ld}), the current in the power grid (i_g) has harmonic content.

To control the AC current, a reference current generation algorithm based on the Fryze Buchholz Depenbrock (FBD) theory was used [31], [32], which is a suitable control theory for single-phase grid connected power converters. In this theory, the converter is modeled by a conductance, consuming a sinusoidal current in phase with the AC voltage. The amplitude of the AC reference current depends upon the operating power, which contains two main components: the power needed to the DC load (p_{dc}) (which can be a direct DC load or through a DC-DC back-end), and the power required to regulate both DC-link voltage (p_{reg}), where a proportional-integral (PI) controller is used. To avoid an oscillation with twice the AC voltage frequency, which is intrinsic to single-phase grid-following power converters, the average values of voltage and current were used for the calculation of the required power. The value of p_{dc} is obtained by the product of the average values of the DC-link voltage (v_{dc2}) with the input current for the DC load (i_{dc}) (or DC-DC back-end converter). Therefore, the AC reference current (i_{USP}*) is obtained according to:

$$i_{USP}{}^{*}(t) = -2\, v_{pll}(t)\, \frac{p_{reg}(t) + p_{dc}(t)}{V_{pk_{pll}}(t)}, \qquad (1)$$

where v_{pll} and V_{pkpll} correspond, respectively, to the fundamental component and to the peak value of the AC voltage. As previously mentioned, the USP front-end converter has as relevant feature the internal division of currents. Thus, FIGURE 4 depicts the inner current separation of the proposed USP front-end converter when operating just as an active rectifier. As expected, i_{USP} is sinusoidal, corresponding to the sum of i_{BAR} with i_{FWR} (i.e., $i_{FWR(d1)}$ when i_{USP} is positive and $i_{FWR(d2)}$ when i_{USP} is negative). As the connection of both internal parts is performed downstream of the AC coupling inductor, these inner currents are switched at high frequency, i.e., the current of the FWR is pulsed with the resulting switching frequency of the BAR. This approach allows to substantially reduce the RMS value of the FWR input current, which contributes to reduce the power losses. Moreover, in this operation mode the DC-link of the BAR (v_{dc1}) supplies power to the DC-link of the FWR (v_{dc2}), regulating simultaneously the average value of both voltages. Since the FWR is a unidirectional topology, the respective DC-link can only provide power to the DC load or DC-DC back-end converter.

However, the arrangement of the BAR and the FWR carries a subtle issue for the integrity of the USP front-end converter when power is being transferred between both DC-links. The operation of the BAR connects in parallel C_1 and C_2, but the existing dead-time between the IGBTs of the same leg causes the disconnection of the two DC-links. As the DC-links are no longer connected in parallel, their voltages will not be balanced. Therefore, when the IGBT switching establishes a new connection between C_1 and C_2, high current spikes can flow in the converter due to the parallel connection of non-equal voltage capacitive elements, which may cause damage to the power semiconductors. This phenomenon occurs in a more intense way when using unipolar pulse-width modulation (PWM) due to the zero-level of the produced voltage. To alleviate this problem, a low value inductor can be connected to interface both BAR and FWR, reducing the current stress and allowing a proper operation of the BAR also with unipolar PWM switching scheme.

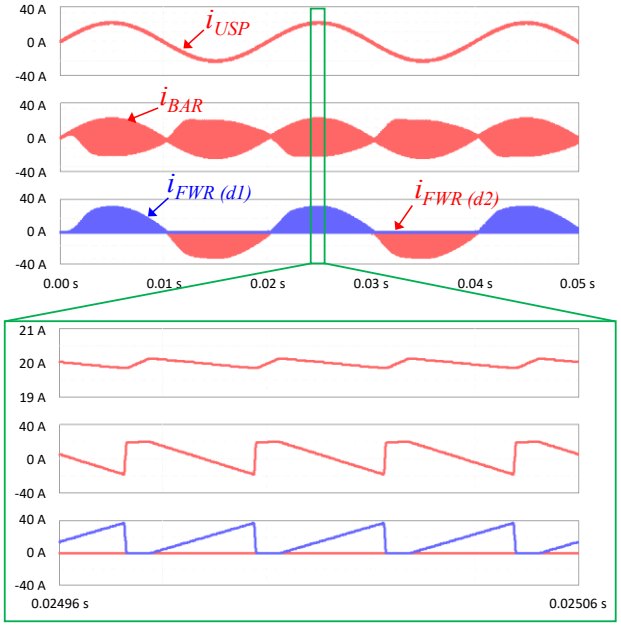

FIGURE 4. Current of the proposed USP front-end converter (i_{USP}) and the internal currents in the BAR (i_{BAR}) and in the FWR (i_{FWR}).

B. Operation Mode: Shunt Active Power Filter

In the previous section, the traditional operation using the proposed USP front-end converter as an active rectifier was introduced. Besides that, as presented before, one of the main advantages of the proposed USP front-end converter is the possibility to operate as a shunt active power filter. This new operation mode consists in controlling the USP front-end converter for compensating current harmonics and reactive power on the power grid side. Consequently, in this operation mode, the exchange of active power between the AC power grid and the DC load is not required, representing an essential asset for supporting power quality. The USP front-end converter operates with non-sinusoidal current to compensate the current harmonics of the non-linear loads connected in the same electrical installation, and consequently, the main current in the power grid is sinusoidal and the power grid only provides active power. This situation is illustrated in FIGURE 5.

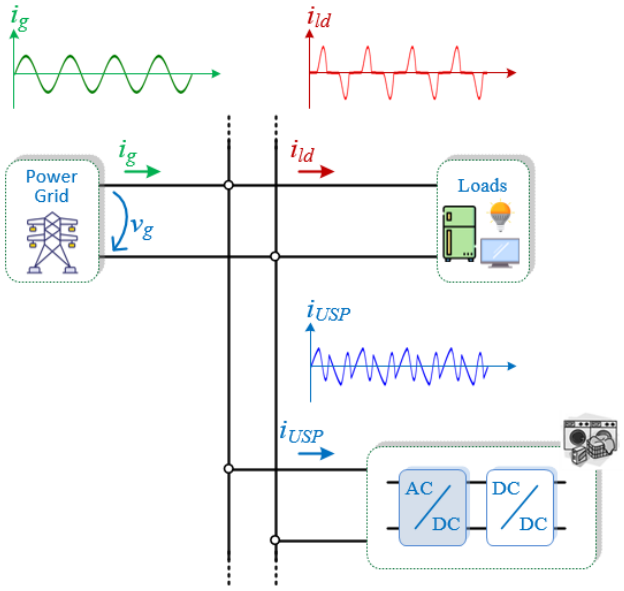

FIGURE 5. Operation mode of the USP front-end converter as shunt active power filter, where it operates with non-sinusoidal current (i_{USP}), and due to its operation, compensating the current harmonic content of the non-linear loads (i_{ld}), the current in the power grid (i_g) becomes sinusoidal.

The AC reference current for the USP front-end converter operating as a shunt active power filter is also obtained with the FBD power theory, which is a largely applied control theory in active power filters. However, in this operation mode, the USP front-end converter cannot be modeled by a conductance, since it must supply the reactive power and harmonic currents demanded by the AC loads connected to the power grid. Instead, the AC loads are modeled by a conductance (meaning the fundamental active power absorbed) connected in parallel with a harmonic current source (meaning the fundamental reactive power and the harmonic currents absorbed by the AC loads). Hence, when operating as a shunt active power filter, the USP front-end converter must operate as a harmonic current source, so the AC power grid is only able to provide fundamental active power (i.e., the harmonic current and reactive power is exchanged just between the USP front-end converter and the AC loads). In this context, the equivalent conductance is also calculated, but since the USP front-end converter does not operate as an active rectifier, the power component p_{dc} is not used. In its place, it is used the active power consumed by the AC loads (p_{ld}), which is calculated by a half-cycle average of the instantaneous load power. It is used only a half-cycle of the AC voltage because it is assumed that the AC loads only absorb odd harmonic currents, which makes the instantaneous load power to have twice the power grid frequency. Besides, the utilization of the half-cycle average instead of the full-cycle version, provides a faster transient response towards AC load changing. To generate the AC reference current when operating as a shunt active power filter, the equivalent conductance current should be subtracted from the loads current (i_{ld}), which results in the harmonic currents and reactive power absorbed by the loads and provided by the USP front-end converter, according to:

$$i_{USP}{}^{*}(t) = i_{ld}(t) - 2\frac{p_{reg}(t)\, v_{pll}(t)}{V_{pk_{pll}}(t)}. \quad (2)$$

Once again, the fundamental component of the AC voltage is used so, due to the operation of the USP front-end converter as a shunt active power filter, the grid current can be sinusoidal with unitary power factor. Contrarily to the operation just as an active rectifier, when the USP front-end converter operates just as a shunt active power filter, the FWR is not used, since its DC-link voltage remains constant with a slightly higher value than the DC-link of the BAR, providing no current flow in the FWR diodes. Hence, the proposed USP front-end converter behaves as a regular AC-DC converter.

C. Operation Mode: Combination of Active Rectifier and Shunt Active Power Filter

The combined operation as an active rectifier and as a shunt active power filter is a relevant operation mode for enhancing power quality in smart grids. The operation mode presented in this section combines the active rectifier process with the shunt active power filter features, i.e., the proposed USP front-end converter operates with a double purpose. In this operation mode, the USP front-end converter operates with non-sinusoidal current to compensate the current harmonics of the non-linear loads connected in the same electrical installation. In addition to the harmonic content, it also presents current in the fundamental frequency of the power grid (50 Hz), ensuring that it operates also with active power. Consequently, the main current in the power grid becomes sinusoidal and the power grid only provides active power, for the loads and for the USP front-end converter. This situation is illustrated in FIGURE 6.

To achieve the combined functionalities, the FBD theory should be modified to encompass both power components p_{dc} and p_{ld}. Like the shunt active power filter operation mode, the USP front-end converter absorbs current with the harmonic content and reactive power required by the AC loads connected to the AC power grid. The only difference lies in its higher amplitude in the combined operation modes, due to the additional power component required, provided by the USP front-end to the DC loads. Thus, the AC reference current calculation is very similar to the shunt active power filter case, which is given by:

$$i_{USP}{}^{*}(t) = i_{ld}(t) - 2v_{pll}(t)\frac{p_{reg}(t) + p_{dc}(t) + p_{ld}(t)}{V_{pk_{pll}}(t)} \quad (3)$$

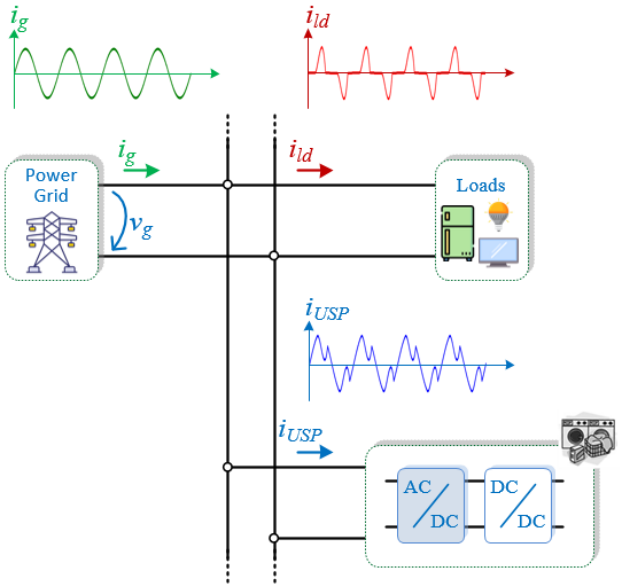

FIGURE 6. Operation mode of the USP front-end converter as a combination of active rectifier and shunt active power filter, where it operates with non-sinusoidal current (i_{USP}), composed by the fundamental frequency of the power grid current (50 Hz) (responsible for ensuring the operation with active power) and by the current harmonics (responsible for compensating the current harmonic content of the non-linear loads (i_{ld})), resulting in a sinusoidal current in the power grid (i_g).

III. PROPOSED DIGITAL CURRENT CONTROL ALGORITHM

The proposed control algorithm, encompassing the distinct operation modes of the proposed USP front-end converter, is presented in this section. A flowchart of the control algorithm is shown in FIGURE 7. As can be seen, the first step consists in reading the different analog to digital converter (ADC) channels. After that, the synchronization with the AC voltage is performed by means of the PLL algorithm and the DC-link voltage is controlled to the established reference average value. According to the operation mode selection (active rectifier; shunt active power filter; or combined active rectifier and shunt active power filter), the AC reference current is established, and the current control is performed through a PWM scheme with a carrier frequency of 20 kHz. The ending process is followed by the start stage to accomplish the selected sampling frequency of 40 kHz.

The PLL algorithm and the DC-link voltage regulation are processed independently of the selected operation mode for the USP front-end converter, since they represent vital elements of the control system of any AC-DC converter connected to the AC power grid. The essential difference between the operation modes consists in the calculated power components used in the equivalent conductance current calculation of the FBD power theory. Hereafter, the current control is processed, so that i_{USP} tracks the attained AC reference properly. For this purpose, it was implemented a predictive-based current control that calculates the reference voltage v_{ab}* (between points a and b identified in FIGURE 1) that is compared with the PWM carrier to obtain the gate-pulse for the IGBTs and, consequently, for producing the current i_{USP} according to its reference. For each given sampling time instant k, the reference voltage v_{ab}* is given by:

$$v_{ab}^*[k] = v_g[k] + \frac{L}{T_s}\left(2i_g^*[k] - i_g^*[k-1] + i_g[k]\right), \quad (4)$$

where v_g denotes the instantaneous value of the AC voltage, L the inductance value of the grid connected coupled inductor and T_s the sampling period.

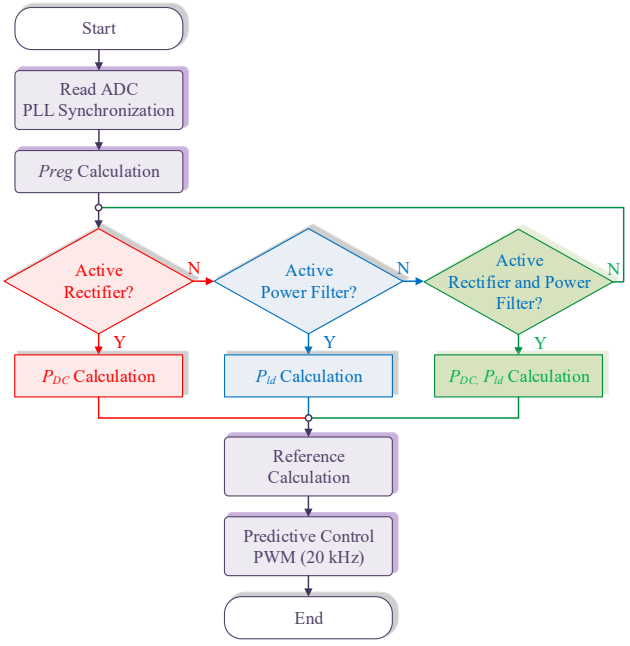

FIGURE 7. Flowchart of the developed control algorithm for the proposed USP front-end converter.

IV. EXPERIMENTAL SETUP AND VALIDATION

The viability of the proposed USP front-end converter was verified with a laboratorial prototype, especially developed for such purpose. A digital signal processor (DSP), with the model TMS320F28335, manufactured by Texas Instruments, was used for digital control implementation. In the conceived power converter, IGBTs with the model FGA25N120N, switched at 20 kHz, and diodes with the model DUR6060W, were used. The DC-link (C_2) is composed by a set of capacitors performing a total capacitance of 1.12 mF (450 V), and the intermediary DC-link (C_1) is composed by a set of capacitors performing a total capacitance of 2.8 mF (450 V). Since the topology of the USP front-end converter allows a bidirectional power flow through the BAR and a unidirectional flow through the FWR, a greater capacity was obtained in the intermediary DC-link (C_1). Thus, for the operation mode as an active rectifier and for the combined operation as an active rectifier and as a shunt

active power filter, the USP front-end converter has a total DC-link capacity resulting from the sum of C_1 and C_2, while in the operation mode just as a shunt active power filter, solely the capacity of C_1 is considered. The USP front-end converter is connected to the AC power grid by means of a coupled inductor with a total value of 2.2 mH. The power converter of the USP front-end converter has a physical size of 17 cm x 17 cm. The digital control system is incorporated into a 1U rack unit, which includes the DSP, the signal conditioning board with external ADC, the external DAC, the control boards for the drivers, and the power supply module (+15 V, GND, -15 V). The prototype was developed for laboratory validation and, therefore, it can be further optimized from an industrial perspective. The laboratorial setup is shown in FIGURE 8. The experimental results were obtained with a digital oscilloscope (Yokogawa model DL708E) and with a power quality analyzer (Fluke, model 435) for the three distinct operation modes: (i) active rectifier; (ii) shunt active power filter; (iii) and active rectifier combined with the shunt active power filter operation.

Although the proposed USP front-end converter was specifically designed for validation under 230 V – 50 Hz conditions, and for a maximum power of 3.6 kW, it has the potential to be adapted for other voltage and power ratings. This would require a revision or replacement of the main components to meet the specific application requirements, which includes the migration for a three-phase version. In such case, it can offer other control advantages to the main power grid, such as the possibility of operating with different values of current harmonics and power factor among the three phases. Regardless of whether a single-phase or three-phase version is used, several USP front-end converters can be combined within the same installation, enabling a modular and scalable solution. This approach can be relevant since it allows the establishment of a dynamic production of selected current harmonics and reactive power. Therefore, according to the availability of the individual USP front-end converters, each one of them can produce selected current harmonics and a specific value of reactive power, with the main goal of ensuring sinusoidal current in the power grid and unitary power factor (e.g., one USP front-end converter can produce 3rd order current harmonics and other one can produce just reactive power). This represents an appealing contribution to power quality management in smart grids.

In the perspective of industrializing the USP front-end converter, it is important the consideration of other components and materials ensuring high efficiency across varying power levels (e.g., by considering wide band gap semiconductors and amorphous/nanocrystalline cores for the L coupling filters). Among other considerations, this analysis must be performed considering the requirements of the final application, the voltage range, and the adaptability to diverse operating conditions (e.g., for thermal management), in order to stablish a trade-off between various power levels and efficiency.

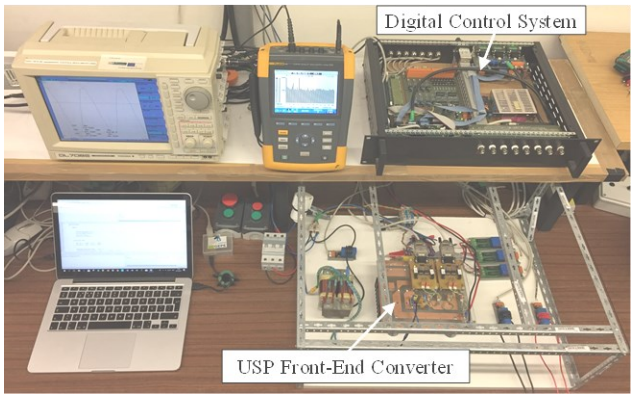

FIGURE 8. Laboratorial setup used to obtain experimental results.

A. Operation Mode: Active Rectifier

FIGURE 9 shows the experimental results of the proposed USP front-end converter, obtained for the operation as an active rectifier for an active power of 1 kW. For the AC side, the AC grid voltage (v_g) and i_{USP} are visible, and for the DC side, this figure shows both DC-link voltages (v_{dc1} and v_{dc2}) and the DC current (i_{dc}) (in the experimental validation a resistive load was considered). As power quality is an important aspect for the AC power grid, during this operation mode, the proposed USP front-end converter operates with unitary power factor and a low total harmonic distortion (THD% = 3.8%) in the controlled i_{USP}. The THD and the spectral analysis of this current are shown in FIGURE 10. FIGURE 11 shows an experimental result during a transient-state, highlighting the moment when the USP front-end begins its operation as active rectifier. In the first stage, it operates as a passive rectifier (i.e., diode bridge) and in the second stage as an active rectifier, where it is demonstrated that the current becomes sinusoidal in the second stage. In addition, due to the operation as active rectifier, the DC-link voltage V_{DC2} also increases.

The proposed control strategy for the USP front-end converter guaranties that the AC grid current is sinusoidal independently of the harmonic distortion of the AC grid voltage, exhibiting a relevant characteristic of the proposed USP front-end converter. As aforementioned, the current separation between the FWR and the BAR is one of the main advantages of the proposed USP front-end converter. FIGURE 12 shows the experimental measure of the i_{BAR} and the i_{USP}, where the BAR current rms value is substantially reduced compared to the AC grid current.

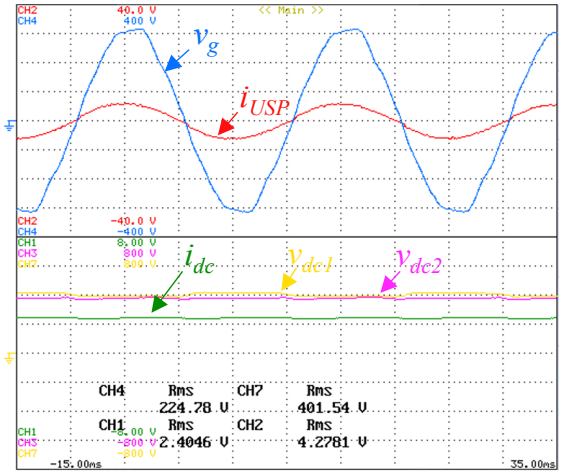

FIGURE 9. Experimental results of the USP front-end converter during the operation as active rectifier: Grid voltage (v_g); USP front-end converter current (i_{USP}); DC-link voltages (v_{dc1} and v_{dc2}); DC current (i_{dc}).

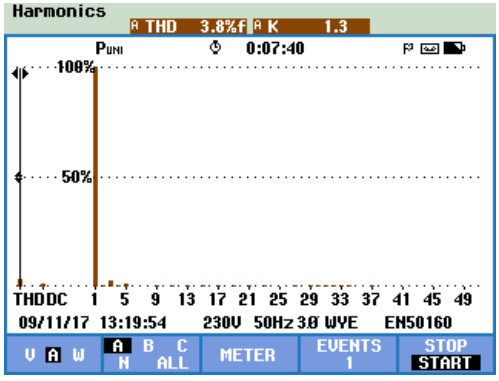

FIGURE 10. Experimental results of the USP front-end converter during the operation as active rectifier: THD and spectral analysis of the current (i_{USP}).

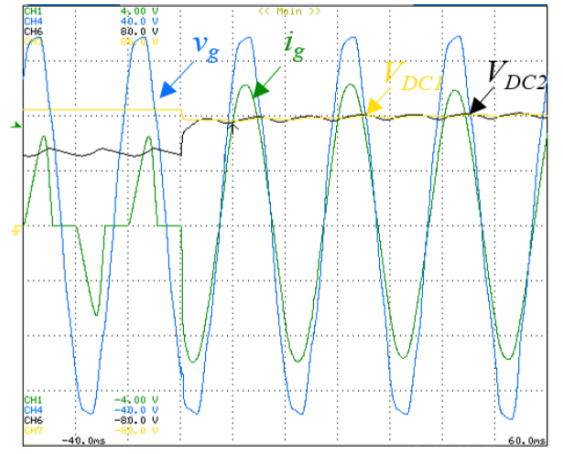

FIGURE 11. Experimental results of the USP front-end converter during the transient-state from the operation as passive rectifier to the operation as active rectifier: Grid voltage (v_g); Grid current (i_g); DC-link voltages (v_{dc1} and v_{dc2}).

B. Operation Mode: Shunt Active Power Filter

To validate the proposed USP front-end converter for the operation as a shunt active power filter, FIGURE 13 shows the current consumed by a non-linear load connected to the AC power grid. The THD and the spectral analysis of the i_{ld} are shown in FIGURE 14.

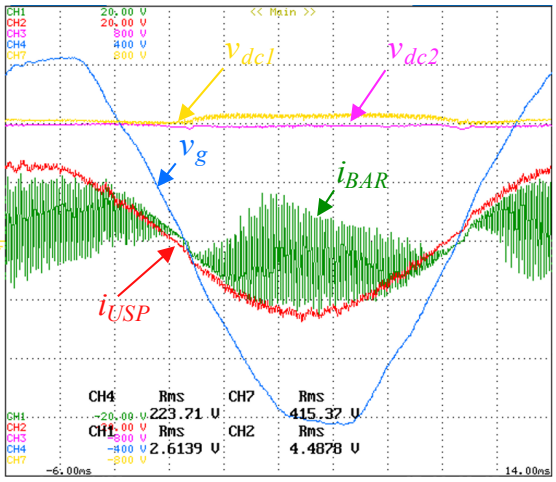

FIGURE 12. Experimental results of the USP front-end converter during the operation as active rectifier: Detail of the BAR current (i_{BAR}) and USP front-end converter current (i_{USP}).

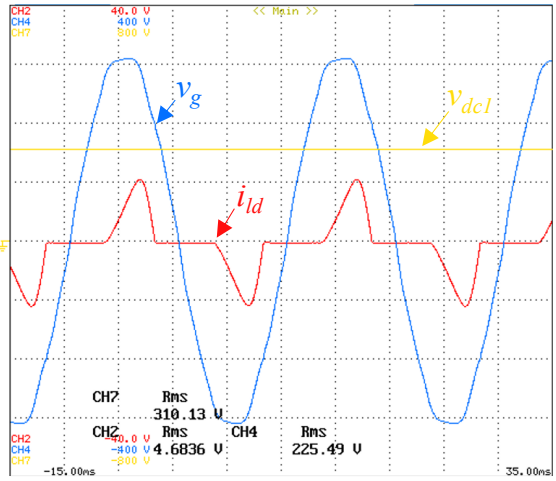

FIGURE 13. Experimental results of the USP front-end converter during the operation as shunt active power filter: Grid voltage (v_g); current consumed by a non-linear load connected to the power grid (i_{ld}); DC-link voltage v_{dc1}.

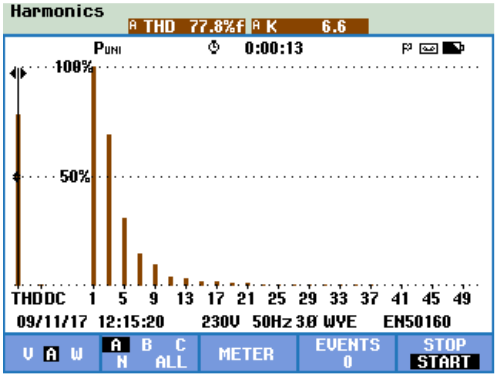

FIGURE 14. Experimental results of the USP front-end converter during the operation as shunt active power filter: THD and spectral analysis of the current consumed by a non-linear load connected to the power grid (i_{ld}).

The i_{USP} can be seen in FIGURE 15, where it is visible that this current has harmonic content in consonance with the harmonic content of the i_{ld}, culminating in a sinusoidal i_g with unitary power factor for the AC power grid side, as it can be seen in FIGURE 16. The THD and the spectral analysis of the AC power grid current (i_g) are shown in FIGURE 17. In this mode, active power between the USP front-end converter and the power grid is not exchanged, but the converter can be used as a dynamic shunt active power filter providing current harmonic compensation for the electrical installation. As a result, the proposed USP front-end converter gives an important contribution to preserve the power quality in smart grids.

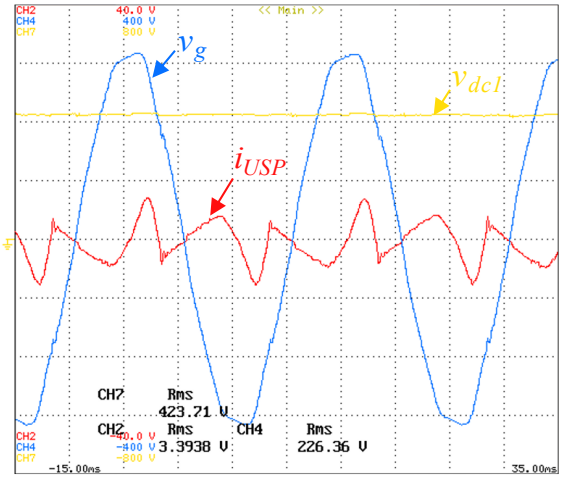

FIGURE 15. Experimental results of the USP front-end converter during the operation as shunt active power filter: Grid voltage (v_g); USP front-end converter current (i_{USP}); DC-link voltage v_{dc1}.

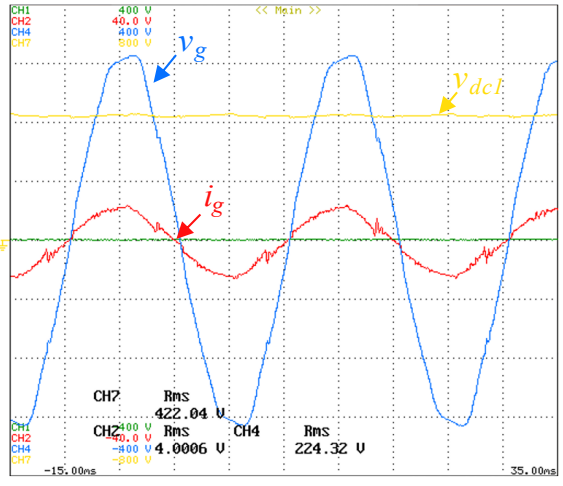

FIGURE 16. Experimental results of the USP front-end converter during the operation as shunt active power filter: Grid voltage (v_g); Grid current (i_g); DC-link voltage v_{dc1}.

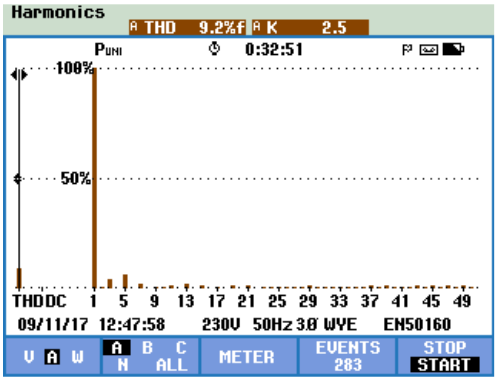

FIGURE 17. Experimental results of the USP front-end converter during the operation as shunt active power filter: THD and spectral analysis of the grid current (i_g).

C. Operation Mode: Combination of Active Rectifier and Shunt Active Power Filter

To validate the combined operation of the proposed USP front-end converter as an active rectifier and as a shunt active power filter, a similar proceeding was used, i.e., a non-linear load was connected to the AC power grid and a resistive load was connected to the DC-link. FIGURE 18 shows, for the AC side, the v_g and the i_g before the operation of the proposed USP front-end converter. For the DC-side, this figure also shows both v_{dc1} and v_{dc2} and the i_{dc}. The THD and spectral analysis of the AC current before the operation of the proposed USP front-end converter can be seen in FIGURE 19.

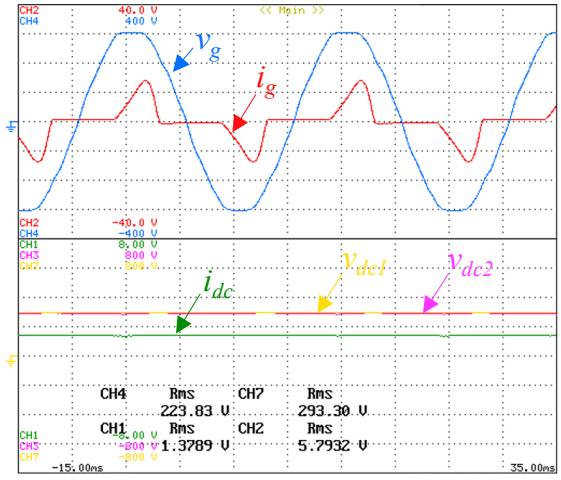

FIGURE 18. Experimental results of the USP front-end converter during the operation as a combination of active rectifier and shunt active power filter: Grid voltage (v_g); Grid current before operation of the proposed USP front-end converter (i_g); DC-link voltages (v_{dc1} and v_{dc2}); DC current (i_{dc}).

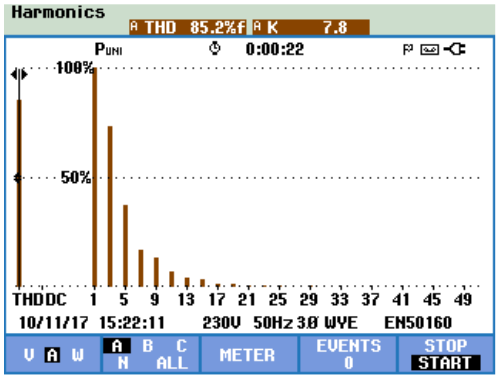

FIGURE 19. Experimental results of the USP front-end converter during the operation as a combination of active rectifier and shunt active power filter: THD and spectral analysis of the grid current before operation of the proposed USP front-end converter (i_g).

FIGURE 20 shows the experimental results of the proposed USP front-end converter for the combined operation as an active rectifier and as a shunt active power filter for an active power of 1.4 kW. The THD and spectral analysis of the i_g can be seen in FIGURE 21. As a result of the operation as a shunt active power filter, the current in the electrical installation is sinusoidal and in phase with the AC grid voltage. In this operation mode, the USP front-end converter operates with adjustable power factor. Moreover, the proposed control strategy guarantees that the i_g is sinusoidal independently of the harmonic distortion of the v_g. Considering that the current separation between the FWR and the BAR is one of the main advantages of the proposed USP front-end converter, FIGURE 22 shows the i_{BAR} and the i_{USP}. Similarly to the previous case, the i_{USP} is distorted for compensating the harmonic content of the i_{ld}, however, it has also a parcel of fundamental component to absorb active power from the AC power grid, which is used to supply the DC load.

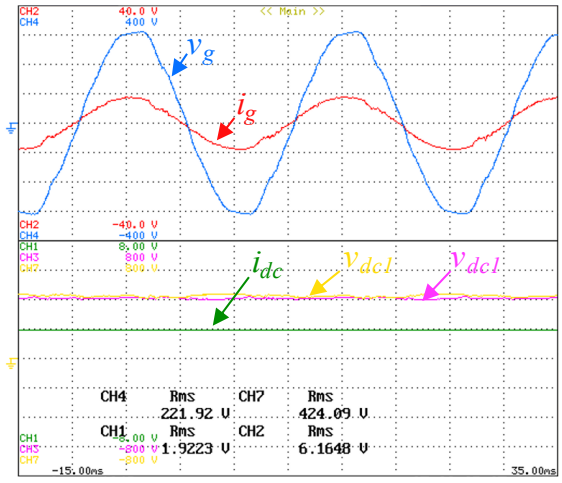

FIGURE 20. Experimental results of the USP front-end converter during the operation as a combination of active rectifier and shunt active power filter: Grid voltage (v_g); Grid current (i_g); DC-link voltages (v_{dc1} and v_{dc2}); DC current (i_{dc}).

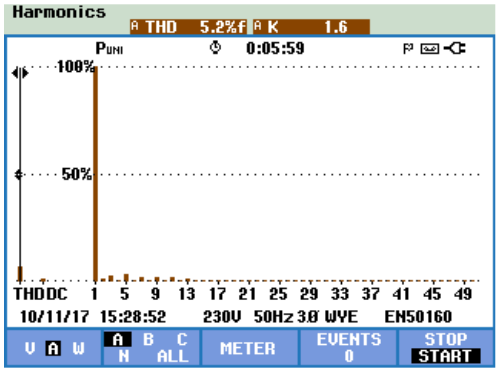

FIGURE 21. Experimental results of the USP front-end converter during the operation as a combination of active rectifier and shunt active power filter: THD and spectral analysis of the grid current (i_g).

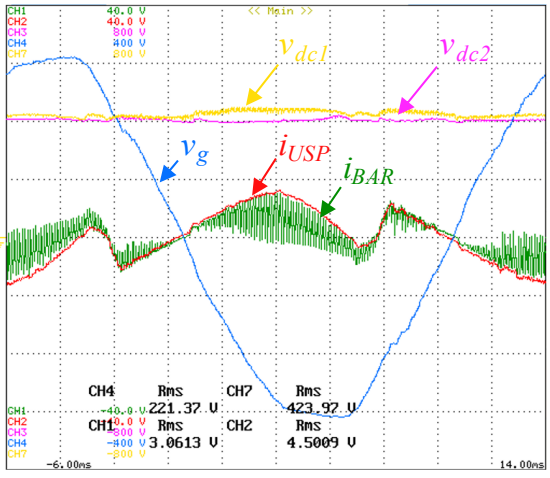

FIGURE 22. Experimental results of the USP front-end converter during the operation as a combination of active rectifier and shunt active power filter: Grid voltage (v_g); USP front-end converter current (i_{USP}); BAR current (i_{BAR}); DC-link voltages (v_{dc1} and v_{dc2}).

The efficiency of the USP front-end converter during the operation in the different modes was carried out by measuring the different operating power levels in the input/output. The results were obtained with the USP front-end converter directly connected to the 230 V AC power grid, but since the operation modes are very distinct, it is not possible to ensure the same power for all scenarios. For such analysis, the Wattmeters model ZIMMER LMG95 and model ISW8000 were considered. The results obtained are summarized in TABLE II.

TABLE II. Efficiency of the USP front-end converter during the operation in the different modes.

Operation Mode	Efficiency
Active Rectifier	92.3%
Shunt Active Power Filter	90.3%
Combination of Active Rectifier and Shunt Active Power Filter	92.7%

V. CONCLUSIONS

A novel unified single-phase (USP) front-end converter is proposed for active rectifiers in smart grids. In addition of ensuring power quality in smart grids, the proposed topology exhibits new functionalities. A laboratorial prototype of 3.6 kW, 230 V – 50 Hz was developed, and experimental results were obtained directly connected to the main AC power grid. The experimental results show the operation as an active rectifier, just ensuring almost sinusoidal AC grid current (THD of 3.8%), unitary power factor, and controlled DC-link voltage. In addition, the experimental validation was also performed with the USP converter operating as a shunt active power filter, where the current presents a harmonic content and controlled power factor, reducing the THD from 77.8% to 9.2%. The combined operation as an active rectifier and as a shunt active power filter was also experimentally verified using a non-linear load with a THD of 85.2%, demonstrating the reduction of the AC grid current THD to 5.2%. In this mode, while operating as shunt active power filter, the USP front-end converter also provides power to the DC load. The experimental results, obtained with the developed prototype, show the feasibility of the topology working in the different operation modes. The proposed unified single-phase active rectifier topology encompasses advanced operating modes that can be an asset in terms of improving power quality for the smart grids.

ACKNOWLEDGMENT

This work has been supported by FCT – Fundação para a Ciência e Tecnologia within the R&D Unit Project Scope UID/00319/Centro ALGORITMI (ALGORITMI/UM). This paper was supported by the Alliance for the Energy Transition (56) co-financed by the Recovery and Resilience Plan (PRR) through the European Union.

REFERENCES

[1] Papalexopoulos, "The Evolution of the Multitier Hierarchical Energy Market Structure: The emergence of the transactive energy model," in *IEEE Electrification Magazine*, vol. 9, no. 3, pp. 37-45, Sept. 2021, doi: 10.1109/MELE.2021.3093598.

[2] R. K. Ahir, B. Chakraborty and P. Mitra, "Informed Change-Point Detection Approach for Solar Prosumer Detection and Statistical Verification in Smart Grid," in *IEEE Transactions on Smart Grid*, vol. 15, no. 1, pp. 987-998, Jan. 2024, doi: 10.1109/TSG.2023.3271219.

[3] M. Khalaf, A. Ayad, M. H. K. Tushar, M. Kassouf and D. Kundur, "A Survey on Cyber-Physical Security of Active Distribution Networks in Smart Grids," in *IEEE Access*, vol. 12, pp. 29414-29444, 2024, doi: 10.1109/ACCESS.2024.3364362.

[4] G. A. Abiassaf and A. A. Arkadan, "Impact of EV Charging, Charging Speed, and Strategy on the Distribution Grid: A Case Study," in *IEEE Journal of Emerging and Selected Topics in Industrial Electronics*, vol. 5, no. 2, pp. 531-542, April 2024, doi: 10.1109/JESTIE.2024.3352505.

[5] Ziyat, A. Gola, P. R. Palmer, S. Makonin and F. Popowich, "EV Charging Profiles and Waveforms Dataset (EV-CPW) and Associated Power Quality Analysis," in *IEEE Access*, vol. 11, pp. 138445-138456, 2023, doi: 10.1109/ACCESS.2023.3340131.

[6] R. K. Lenka, A. K. Panda, R. Patel and J. M. Guerrero, "PV Integrated Multifunctional Off-Board EV Charger With Improved Grid Power Quality," in *IEEE Transactions on Industry Applications*, vol. 58, no. 5, pp. 5520-5532, Sept.-Oct. 2022, doi: 10.1109/TIA.2022.3167659.

[7] N. Kumar, V. Saxena, B. Singh and B. K. Panigrahi, "Power Quality Improved Grid-Interfaced PV-Assisted Onboard EV Charging Infrastructure for Smart Households Consumers," in *IEEE Transactions on Consumer Electronics*, vol. 69, no. 4, pp. 1091-1100, Nov. 2023, doi: 10.1109/TCE.2023.3296480.

[8] R. K. Lenka, A. K. Panda, A. R. Dash, L. Senapati and N. Tiwary, "A Unified Control of Grid-Interactive Off-Board EV Battery Charger with Improved Power Quality," in *IEEE Transactions on Transportation Electrification*, vol. 9, no. 1, pp. 920-933, March 2023, doi: 10.1109/TTE.2022.3172354.

[9] S. S. Sayed and A. M. Massoud, "Review on State-of-the-Art Unidirectional Non-Isolated Power Factor Correction Converters for Short-/Long-Distance Electric Vehicles," in *IEEE Access*, vol. 10, pp. 11308-11340, 2022, doi: 10.1109/ACCESS.2022.3146410.

[10] A. Abdel-Aziz, M. A. Elgenedy and B. W. Williams, "Two-Leg Neutral-Point Diode-Clamped Active Front-End Rectifier," in *IEEE Journal of Emerging and Selected Topics in Power Electronics*, vol. 12, no. 1, pp. 405-419, Feb. 2024, doi: 10.1109/JESTPE.2023.3336571.

[11] H. Zhang, H. Li, J. Mao, C. Pan and Z. Luan, "Model-Free Control of Single-Phase Boost AC/DC Converters," in *IEEE Transactions on Power Electronics*, vol. 37, no. 10, pp. 11828-11838, Oct. 2022, doi: 10.1109/TPEL.2022.3176937.

[12] G. K. N. Kumar, A. K. Verma, S. N and K. Shukla, "A Single-Stage Boost Derived Switched-Capacitor- Based PFC Converter for EV Applications," in *IEEE Journal of Emerging and Selected Topics in Industrial Electronics*, vol. 5, no. 1, pp. 225-233, Jan. 2024, doi: 10.1109/JESTIE.2023.3341772.

[13] J. -W. Yang and H. -L. Do, "Single-Stage Two-Flyback PFC Converter With Low Voltage Stress on a Switch," in *IEEE Transactions on Industrial Electronics*, vol. 72, no. 2, pp. 1466-1474, Feb. 2025, doi: 10.1109/TIE.2024.3429651.

[14] Y. He, J. Hu, C. Shen and L. Hang, "A Cascaded Bridgeless Boost PFC With Low Common-Mode Noise," in *IEEE Transactions on Power Electronics*, vol. 39, no. 5, pp. 4969-4973, May 2024, doi: 10.1109/TPEL.2024.3356588.

[15] S. Sharifi, M. Monfared and M. Babaei, "Ferdowsi Rectifiers—Single-Phase Buck-Boost Bridgeless PFC Rectifiers with Low Semiconductor Count," in *IEEE Transactions on Industrial Electronics*, vol. 67, no. 11, pp. 9206-9214, Nov. 2020, doi: 10.1109/TIE.2019.2955430.

[16] Z. Chen, B. Liu, Y. Yang, P. Davari and H. Wang, "Bridgeless PFC Topology Simplification and Design for Performance Benchmarking," in *IEEE Transactions on Power Electronics*, vol. 36, no. 5, pp. 5398-5414, May 2021, doi: 10.1109/TPEL.2020.3028419.

[17] M. Cirrincione, M. Pucci and G. Vitale, "A Single-Phase DG Generation Unit with Shunt Active Power Filter Capability by Adaptive Neural Filtering," in *IEEE Transactions on Industrial Electronics*, vol. 55, no. 5, pp. 2093-2110, May 2008, doi: 10.1109/TIE.2008.918642.

[18] S. Devassy and B. Singh, "Implementation of Solar Photovoltaic System with Universal Active Filtering Capability," in *IEEE Transactions on Industry Applications*, vol. 55, no. 4, pp. 3926-3934, July-Aug. 2019, doi: 10.1109/TIA.2019.2906297.

[19] S. Devassy and B. Singh, "Control of a Solar Photovoltaic Integrated Universal Active Power Filter Based on a Discrete Adaptive Filter," in *IEEE Transactions on Industrial Informatics*, vol. 14, no. 7, pp. 3003-3012, July 2018, doi: 10.1109/TII.2017.2778346.

[20] M. A. Mansor, K. Hasan, M. M. Othman, S. Z. B. M. Noor and I. Musirin, "Construction and Performance Investigation of Three-Phase Solar PV and Battery Energy Storage System Integrated UPQC," in *IEEE Access*, vol. 8, pp. 103511-103538, 2020, doi: 10.1109/ACCESS.2020.2997056.

[21] T. Soeiro, T. Friedli and J. W. Kolar, "Three-phase high power factor mains interface concepts for Electric Vehicle battery charging systems," Twenty-Seventh Annual *IEEE Applied Power Electronics Conference and Exposition* (APEC), Orlando, FL, USA, 2012, pp. 2603-2610, doi: 10.1109/APEC.2012.6166190.

[22] V. Monteiro et al., "A Novel Three-Phase Multiobjective Unified Power Quality Conditioner," in IEEE Transactions on Industrial Electronics, vol. 71, no. 1, pp. 59-70, Jan. 2024, doi: 10.1109/TIE.2023.3241380.
[23] M. Golla, S. Thangavel, S. P. Simon and N. P. Padhy, "An Enhancement of Power Quality With Efficient Active Power Transfer Capability in a PV–BSS-Fed UAPF for Microgrid Realization," in IEEE Systems Journal, vol. 17, no. 1, pp. 1614-1625, March 2023, doi: 10.1109/JSYST.2022.3179182.
[24] M. Golla, S. Thangavel, S. P. Simon and N. P. Padhy, "A Novel Control Scheme Using UAPF in an Integrated PV Grid-Tied System," in IEEE Transactions on Power Delivery, vol. 38, no. 1, pp. 133-145, Feb. 2023, doi: 10.1109/TPWRD.2022.3180681.
[25] G. K. Reddy, G. B. Kumbhar and N. P. Padhy, "An Extended Partial Harmonic Current Compensation for Multifunctional PV Inverters," 2023 IEEE International Conference on Power Electronics, Smart Grid, and Renewable Energy (PESGRE), Trivandrum, India, 2023, pp. 1-6, doi: 10.1109/PESGRE58662.2023.10404793.
[26] A. Amirullah and A. Adianandа, "Dual Fuzzy-Sugeno Method to Enhance Power Quality Performance Using a Single-Phase Dual UPQC-Dual PV Without DC-Link Capacitor," in Protection and Control of Modern Power Systems, vol. 9, no. 1, pp. 133-153, January 2024, doi: 10.23919/PCMP.2023.000107.
[27] A. Kazemtarghi, A. Chandwani, N. Ishraq and A. Mallik, "Active Compensation-Based Harmonic Reduction Technique to Mitigate Power Quality Impacts of EV Charging Systems," in IEEE Transactions on Transportation Electrification, vol. 9, no. 1, pp. 1629-1640, March 2023, doi: 10.1109/TTE.2022.3183478.
[28] V. Jain, S. Kewat and B. Singh, "Three Phase Grid Connected PV Based EV Charging Station With Capability of Compensation of Reactive Power," in IEEE Transactions on Industry Applications, vol. 59, no. 1, pp. 367-376, Jan.-Feb. 2023, doi: 10.1109/TIA.2022.3213530.
[29] R. K. Lenka, A. K. Panda, R. Patel and J. M. Guerrero, "PV Integrated Multifunctional Off-Board EV Charger With Improved Grid Power Quality," in IEEE Transactions on Industry Applications, vol. 58, no. 5, pp. 5520-5532, Sept.-Oct. 2022, doi: 10.1109/TIA.2022.3167659.
[30] M. Karimi-Ghartemani, "Linear and Pseudolinear Enhanced Phased-Locked Loop (EPLL) Structures," in *IEEE Transactions on Industrial Electronics*, vol. 61, no. 3, pp. 1464-1474, March 2014, doi: 10.1109/TIE.2013.2261035.
[31] M. Depenbrock, "The FBD-method, a generally applicable tool for analyzing power relations," in *IEEE Transactions on Power Systems*, vol. 8, no. 2, pp. 381-387, May 1993, doi: 10.1109/59.260849.
[32] Staudt, "Fryze - Buchholz - Depenbrock: A time-domain power theory," 2008 *International School on Nonsinusoidal Currents and Compensation*, Lagow, Poland, 2008, pp. 1-12, doi: 10.1109/ISNCC.2008.4627481.

Vitor Monteiro (SM, IEEE) received the Ph.D. degree in Power Electronics and Energy Systems in 2016, and the M.Sc. in Industrial Electronics and Computer Engineering in 2010, both from the University of Minho, Portugal. Currently, he is an Assistant Professor at the Department of Industrial Electronics, University of Minho, Portugal. His research activity has been developed at the Group of Energy and Power Electronics (GEPE), in the fields of industrial and power electronics, electric mobility, renewables, and power quality.

Filipe Costa received the M.Sc. degree in Power Electronics and Energy Systems in 2017 from the School of Engineering of the University of Minho, Portugal. His final M.Sc. dissertation was about the design and development of a unified EV battery charging system with active power filter features. Nowadays, he is a professional of power electronics for electric mobility.

Sergio Coelho (S) received the M.Sc. degree in Power Electronics and Energy Systems in 2019 from the School of Engineering of the University of Minho, Portugal, where he is currently pursuing a Ph.D. focused on new power electronics technologies for solid-state transformers. His main interests are related to power electronics, solid-state transformers, hybrid AC/DCpower grids, and renewable energy sources.

João L. Afonso (SM, IEEE) is Full Professor of the Department of Industrial Electronics, University of Minho, Portugal. He received the B.Sc. and M.Sc. degrees in Electrical Engineering from the Federal University of Rio de Janeiro, Brazil, in 1986 and 1991, and the Ph.D. degree in Industrial Electronics from the University of Minho, in 2000. He has been with the Department of Industrial Electronics of the University of Minho since 1993. He is coordinator and researcher with the Group of Energy and Power Electronics (GEPE).